Available online at www.sciencedirect.com
ScienceDirect
Natural Gas Industry B 6 (2019) 629−638
www.keaipublishing.com/en/journals/natural-gas-industry-b/

Research Article

Novel mathematical correlation for accurate prediction of gas compressibility factor

Ekechukwu Gerald Kelechi [a,*] & Orodu Oyinkepreye David [b]

[a] Department of Petroleum Engineering, University of Wyoming, 82072, United States
[b] Department of Petroleum Engineering, Covenant University, Ota, Ogun State, Nigeria

Received 9 September 2019; accepted 16 September 2019
Available online 6 December 2019

Abstract

Gas compressibility factor is a critical thermodynamic property that is a required input in the estimation of many reservoir fluid properties and reservoir engineering calculations. Experimentally derived values are considered the best, but these are very expensive and time-consuming. In this work, we have developed a new simplified explicit compressibility factor correlation based on a large dataset using a hybrid nonlinear optimization technique. The new model has a correlation coefficient of 0.9997 and very low average relative error and root-mean-square errors. Statistical analysis shows that this new correlation outperforms all of the existing correlations within the range of $0.2 < Ppr < 15$ and $1.05 < Tpr < 2$).

Keywords: Compressibility factor; Empirical model; Explicit correlation; Pseudo-critical properties

1. Introduction

The demand for natural gas has risen continually in recent years due to its notable capacity of burning without any environmentally damaging footprint. This growing significance has prompted the need for more efficient and accurate characterization of natural gas properties and reserves. The accurate and reliable estimations of most gas properties, such as formation volume factor, gas viscosity, gas density, and gas compressibility are heavily dependent on the accuracy of the compressibility factor [1]. Gas compressibility factor is an important parameter in natural gas reserves assessment and many reservoir fluid properties estimations. In the petroleum industry, some calculations such as gas reservoir performance forecasting, initial gas in place, future production of gas prediction, as well as gas reserve estimation are done with these gas properties. Many oil and gas companies, as well as the government, require these accurate gas field assessments for better decision making when diverse investment portfolios exist.

Well-conducted laboratory procedures give the best estimates of fluid properties and are considered as the standard approach. These experimental procedures are, however, too costly and time-consuming. Empirical correlations and equation of state approaches have been employed over time for relatively faster and cheaper determination of compressibility factor [2−7]. However, correlations are commonly used because they are faster than the equation of state approach. Most of the empirical correlations are based on the law of corresponding states. This law posits that the same z-factor is assigned to substances that have the same conditions obtained by using their critical temperature and critical pressure to normalize the reservoir's temperature and pressure. The formula for the reduced pressure (Pr) and temperature (Tr) are obtained using Eqns (1) and (2) below:

* Corresponding author.
E-mail address: geraldekechukwu@gmail.com (Ekechukwu G.K.).
Peer review under responsibility of Sichuan Petroleum Administration.

https://doi.org/10.1016/j.ngib.2019.09.001
2352-8540/

$$P_r = \frac{P}{P_c} \tag{1}$$

$$Tr = \frac{T}{T_c} \tag{2}$$

The pseudocritical pressure (P_{pc}) and temperature (T_{pc}) are required for natural gas streams, hence, knowledge of either the gas gravity or gas compositions are needed to estimate these critical properties of natural gas. In addition, several mixing rules have been proposed from which the equivalent critical properties of natural gases can be estimated. Kay's mixing rule [8], Stewart-Burkhart-Voo [9], Sutton- Stewart-Burkhart-Voo [10] and Corredor et al., [11] mixing rules are amongst the most popular ones.

Non-hydrocarbon components are sometimes present in the gas streams; this thereby warrants that the pseudo-critical properties are adjusted by a simple procedure developed by Carr, Kobayashi, and Burrows [12]. The correlations presented by Wichert and Aziz [13] are used to correct for the non-hydrocarbon impurities in natural gases such as CO_2 and H_2S.

In this work, a novel, simple, robust and accurate explicit correlation from a large published database is proposed. This correlation is considered as simple because it has just 13 parameters which are way lower than what we have in other explicit correlations. It is considered as robust and accurate because it works excellently well at estimating the z-factors at a wide range of application ($0.2 < Ppr < 15$ and $1.05 < Tpr < 2$). Besides, statistical analysis shows that this new correlation outperforms most of the existing correlations.

2. Generalized empirical correlations

Five alternative explicit correlations have been presented in this study for the purpose of comparison. The first correlation presented is a classic explicit correlation that has an acceptable degree of accuracy within a certain range of application. The second correlation presented was developed by a famous oil and gas company and the main purpose of including this correlation is to show how important this thermodynamic property is to the energy industry. Also presented are three recent correlations that have attempted to increase the accuracy of the explicit correlations. More details of the correlations are given below.

2.1. Beggs and Brill [5]

Beggs and Brill [5] proposed a best−fit equation for the Standing and Katz [22] z-factor Chart.

The correlation is as follows:

$$z = A + \frac{(1-A)}{e^B} + CP_{pr}^D \tag{3}$$

where,

$$A = 1.39\left(T_{pr} - 0.92\right)^{0.5} - 0.36T_{pr} - 0.101$$

$$B = (0.62 - 0.23)P_{pr} + \left[\frac{0.066}{\left(T_{pr} - 0.86\right)} - 0.037\right]P_{pr}^2 + \frac{0.32}{10^{9\left(T_{pr}-1\right)}}P_{pr}^6$$

$$C = \left(0.132 - 0.32 logT_{pr}\right)$$

$$D = 10^{\left(0.3016 - 0.49T_{pr} + .1824T_{pr}^2\right)}$$

2.2. Shell Oil company fitting equation [21]

Shell Oil company also provided a best−fit equation as shown below [21].

$$Z = ZA + ZB\ x\ P_{pr} + (1 - ZA)\ x\ EXP\ (-ZG)\ x\ \left(\frac{p_{pr}}{10}\right)^4 \tag{4}$$

where

$$ZA = -0.101 - 0.36\ x\ T_{pr} + 1.3868\ x\ \sqrt{\left(T_{pr} - 0.919\right)}$$

$$ZB = 0.021 + \frac{0.04275}{\left(T_{pr} - 0.65\right)}$$

$$ZC = 0.6222 - 0.224\ x\ T_{pr}$$

$$ZD = \frac{0.0657}{\left(T_{pr} - 0.86\right)} - 0.037$$

$$ZE = 0.32\ x\ EXP\ \left(-19.53\ x\ \left(T_{pr} - 1\right)\right)$$

$$ZF = 0.122\ x\ EXP\ \left(-11.3\ x\ \left(T_{pr} - 1\right)\right)$$

$$ZG = P_{pr}\ x\ \left(ZC + ZD\ x\ P_{pr} + ZE\ x\ P_{pr}^4\right)$$

2.3. Kareem et al. [4]

Kareem et al. [4] based on Hall and Yarborough's implicit correlation, developed an explicit Correlation from 5346 experimental data points. The details are presented below:

$$z = \frac{DP_{pr}\left(1 + y + y^2 - y^3\right)}{\left(DP_{pr} + Ey^2 - Fy^G\right)(1 - y)^3} \tag{5}$$

$$y = \frac{DP_{pr}}{\left(\frac{1+A^2}{C} - \frac{A^2B}{C^3}\right)} \tag{6}$$

where

$$t = \frac{1}{T_{pr}}$$

$$A = a_1 t e^{a_2(1-t)^2} P_{pr}$$

$$B = a_3 t + a_4 t^2 + a_5 t^6 P_{pr}^6$$

$$C = a_9 + a_8 t P_{pr} + a_7 t^2 P_{pr}^2 + a_6 t^3 P_{pr}^3$$

$$D = a_{10} t e^{a_{11}(1-t)^2}$$

$$E = a_{12} t + a_{13} t^2 + a_{14} t^3$$

$$F = a_{15} t + a_{16} t^2 + a_{17} t^3$$

$$G = a_{18} + a_{19} t$$

Coefficients	Estimated Values
a1	0.317842
a2	0.382216
a3	−7.76835
a4	14.2905
a5	2.18363E-06
a6	−0.00469257
a7	0.0962541
a8	0.16672
a9	0.96691
a10	0.063069
a11	−1.966847
a12	21.0581
a13	−27.0246
a14	16.23
a15	207.783
a16	−488.161
a17	176.29
a18	1.88453
a19	3.05921

2.4. Kamari et al. [23]

Kamari et al. [23] used the gene expression programming mathematical approach to develop a new correlation for the determination of the gas compressibility of around 900 data points.

$$Z = 0.2625136 + \frac{3.1263651}{T_{pr}} + \frac{-3.8916368}{T_{pr}^2} + \frac{1.0551763}{T_{pr}^3} + 0.5638878\left[In\left(P_{pr}\right)\right] - 0.3372525\left[In\left(P_{pr}\right)\right]^2 + 0.061688\left[In\left(P_{pr}\right)\right]^3 + \frac{-1.3976452\left[In\left(P_{pr}\right)\right]}{T_{pr}} + \frac{0.5217521\left[In\left(P_{pr}\right)\right]}{T_{pr}^2} + \frac{0.447935\left[In\left(P_{pr}\right)\right]^2}{T_{pr}} \tag{7}$$

2.5. Azizi et al. [3]

Azizi et al. [3] proposed a new correlation that is developed from 4158 experimental z-values that are extracted from the Standing and Katz chart ($0.2 < Pr < 15$ and $1.1 < Tr < 2$). This correlation was an improvement over the lead author's previous correlation [2] that covered a reduced range of $0.2 < Pr < 11$ and $1.1 < Tr < 2$.

$$Z = 1 + P_r\left(\frac{A+B}{C+D}\right) \tag{8}$$

where:

$$A = 1 + aT_r^{-0.5} + bP_r^{0.5} + cT_r^{-1.3}P_r^{2.4}$$

$$B = dIn(T_r) + e[In(T_r)]^{0.001} + f[In(T_r)]^{0.2} + gIn(P_r) + h[In(P_r)]^2 + i[In(P_r)]^3 + jIn(T_r)In(P_r) + k[In(T_r)]^{0.2}In(P_r) + l[In(T_r)]^{-1.3}[In(P_r)]^2$$

$$C = 1 + mP_r^{1.957} + nT_r^{0.6}P_r^{0.68}$$

$$D = oIn(T_r) + p[In(T_r)]^{0.3} + qIn(P_r) + r[In(P_r)]^2 + s[In(T_r)]^{2.3}In(P_r)$$

Coefficients	Tuned Values
a	3.54875035417288
b	−4.21664513837899
c	−4.10613526239254E-03

(continued on next page)

(*continued*)

Coefficients	Tuned Values
d	0.28144444316384
e	−1.58050421246329
f	2.39137824393016
g	2.10533680903090
h	0.57558851625008
i	0.10884774149922
j	−0.28097160193372
k	0.13571880130394
l	1.76679767712678E-03
m	−0.20648400338479
n	−0.24728491152373
o	−0.69181729576201
p	−5.33433422937078
q	0.59152637120218
r	0.22394631804226
s	−0.56024088109368

3. Methodology

3.1. Database

The newly proposed correlation was developed from a large database containing 4455 data points. The data was published by Poettmann and Carpenter [14] as a digitized version of the Standing and Katz [22] (S−K) chart, displayed in Fig.1. Table 1 shows the statistical properties of the S−K data, which may be otherwise referred to as experimental data.

3.2. Model development

A new explicit compressibility factor correlation based on the above-mentioned standard data is presented. The functional form of this equation is quite different from those of the existing correlations. The initial parameters were first generated using the Levenberg-Marquart Algorithm (LMA) technique [15−17]. The LMA is an iterative optimization technique that interpolates between the Gauss-Newton algorithm (GNA) and the method of gradient descent [15]. The LMA is a very strong algorithm that has been used for parameter optimization in several artificial intelligence algorithms such as artificial neural networks and adaptive neuro-fuzzy inference systems (ANFIS) [3,18].

Given a set of n empirical data points $(Ppr_i,\ Tpr_i,\ z_i)$ of independent and dependent variables, the algorithm attempts to find the vector of parameter $\hat{a}$ of the model curve $f(Ppr_i,\ Tpr_i,\ \beta)$ so that the sum of the squares of the deviations is minimized.

Table 1
Statistical details of the 4455 data points used in this study as published by Poetmann and Carpenter [14].

	Ppr	Tpr	Z
Mean	7.6	1.45	1.03116
Minimum	0.2	1.05	0.251
Median	7.6	1.4	0.987
Maximum	15	2	1.753
Standard Deviation	4.28728	0.28581	0.28363
Skewness	−1.08361E-15	0.45006	0.07414
urtosis	−1.20003	−0.93294	−0.43937
Geometric SD	2.39595	1.21407	1.35203
Mode	0.2	1.05	0.937
Harmonic Mean	3.33758	1.39664	0.9406

$$\widehat{\beta} = argmin_{\beta} \sum_{i=1}^{n} \left[z_i - f(Ppr_i,\ Tpr_i,\ \beta)\ \right]^2 \tag{9}$$

The LMA is an iterative process in which at each iteration step, the vector of parameter β is replaced by a new estimate $\beta + \delta$. The δ is approximated by linearizing the function as follows:

$$f(Ppr_i,\ Tpr_i,\ \beta+\delta)\ \approx f(Ppr_i,\ Tpr_i,\ \beta) + \boldsymbol{J}_i\delta_i \tag{10}$$

where $\boldsymbol{J_i}$ is the differential of model function with respect to the vector of parameter β. It may be otherwise called the Jacobian of the function f.

The results of the parameters given by the LMA, however, gave a poor prediction. This could be attributed to the fact that the LMA typically finds a local minimum, which may not necessarily be the global minimum. To further optimize the parameterization, we used the orthogonal distance non-linear regression (ODR) technique to obtain an updated $\widehat{\beta}$ [19,20]. The ODR technique adds another noise term ε to the model equation.

$$z_i = f(Ppr_i,\ Tpr_i,\ \beta) + \varepsilon_i \tag{11}$$

The updated parameter vector is then obtained by minimizing both $\widehat{\beta}$ and ε in the following equation:

$$\widehat{\beta} = argmin_{\beta,\varepsilon} \sum_{i=1}^{n} \left[z_i - f(Ppr_i,\ Tpr_i,\ \delta_i\ ,\beta)\ \right]^2 + \delta_i^2 \tag{12}$$

The main objective of the orthogonal distance regression (ODR), is to minimize the sum of squares of orthogonal Euclidean distances from data points to the fitting curve as shown in equation (12), hence getting a better prediction [19].

The hybrid optimization technique has resulted in a simple correlation with just 13 parameters and no additional derived parameters. It takes the functional form as shown in equation (13) below with only the pseudocritical pressures and temperatures as input:

$$z = \frac{a0 + a1{*}P_{pr} + a2{*}y^{1.1} + a3{*}y^{2.75} + a4{*}\ y^{3} + a5{*}y^{0.15}}{1 + a6{*}P_{pr} + a7{*}P_{pr}^{2.2} + a8{*}\ P_{pr}^{3.75} + a9{*}y^{0.89} + a10{*}\ y^{2.05} + a11{*}y^{2.2} + a12{*}P_{pr}^{0.2}} \tag{13}$$

where $y = P_{pr}/T_{pr}$

Table 2 shows the optimized coefficients obtained from the hybrid optimization technique used in this study.

3.3. Performance evaluators

Statistical metrics are used to validate the accuracy and reliability of the newly developed correlation.

The statistical measures used are described below:

3.3.1. Correlation coefficient

The formula is defined below:

$$R = \sqrt{1 - \sum_{i=1}^{n}\left[x_{S-K} - x_{est}\right]_i^2 \Big/ \sum_{i=1}^{n}\left[x_{S-K} - \underline{x}\right]^2} \tag{14}$$

where, $\underline{x} = \frac{1}{n}\sum_{i=1}^{n}[x_{S-K}]$

3.3.2. Average absolute percentage error (AAPE)

$$E_a = \frac{100}{n}\sum_{i=1}^{n}\left|\frac{x_{S-K} - x_{est}}{x_{S-K}}\right| \tag{15}$$

3.3.3. Maximum absolute percentage relative error

Apart from the absolute percent relative error for each data, the maximum values are also useful in that they are used to know the range of error for each correlation:

$$E_{max} = max_{i=1}^{n}\left|\frac{x_{S-K} - x_{est}}{x_{S-K}}\right| * 100 \tag{16}$$

3.3.4. Root mean square error

Mathematically described below;

$$RMSE = \sqrt{\sum_{i=1}^{n}\frac{\left(x_{S-K} - x_{est}\right)^2}{n}} \tag{17}$$

Root mean square error always give a non-negative output, with the value of zero indicating a perfect match with the data.

3.3.5. Sum of squared error of prediction (SSE)

$$SSE = \sum_{i=1}^{n}\left(x_{est} - x_{S-K}\right)^2 \tag{18}$$

Table 2
Optimized coefficients for the new correlation.

Coefficients	Mean estimate
a0	2.409560927
a1	1.488390466
a2	−1.585509276
a3	0.216944783
a4	−0.103474667
a5	−2.275620224
a6	1.45660194
a7	−0.026764378
a8	0.000112856
a9	−2.632236075
a10	1.491950114
a11	−0.939533875
a12	−8.62E-10

Table 3
Statistical comparison between experimental and predicted data.

	Actual Data	Predicted Data
Mean	1.02078	1.02081
Standard Deviation	0.27765	0.27744
Skewness	0.13383	0.13379
Kurtosis	−0.27731	−0.26918
Mean absolute Deviation	0.22359	0.22326
Geometric Mean	0.98001	0.98009
Minimum	0.251	0.26277
Median	0.977	0.97739
Maximum	1.753	1.76713
Interquartile Range (Q3 - Q1)	0.379	0.37894
Median Absolute Deviation	0.185	0.18448

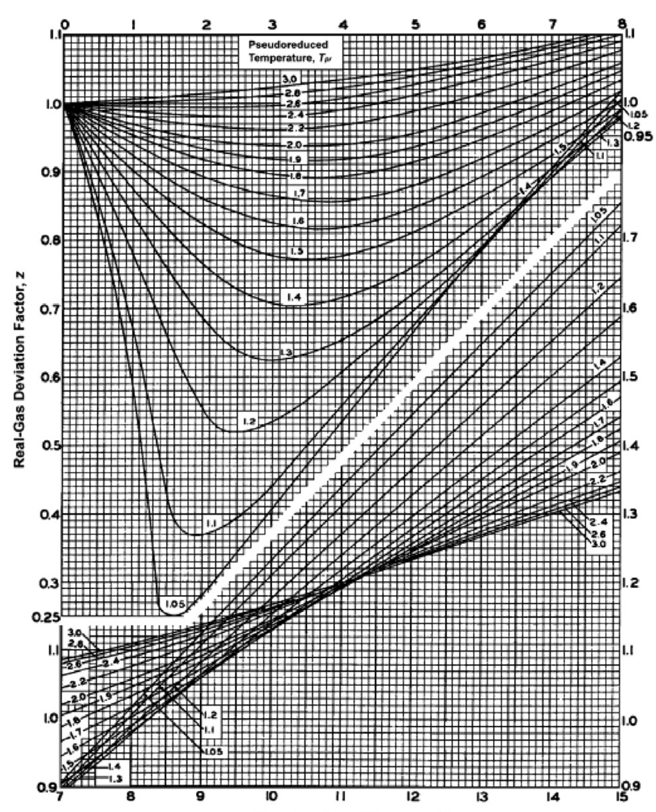

Fig. 1. Original standing and katz [22] chart.

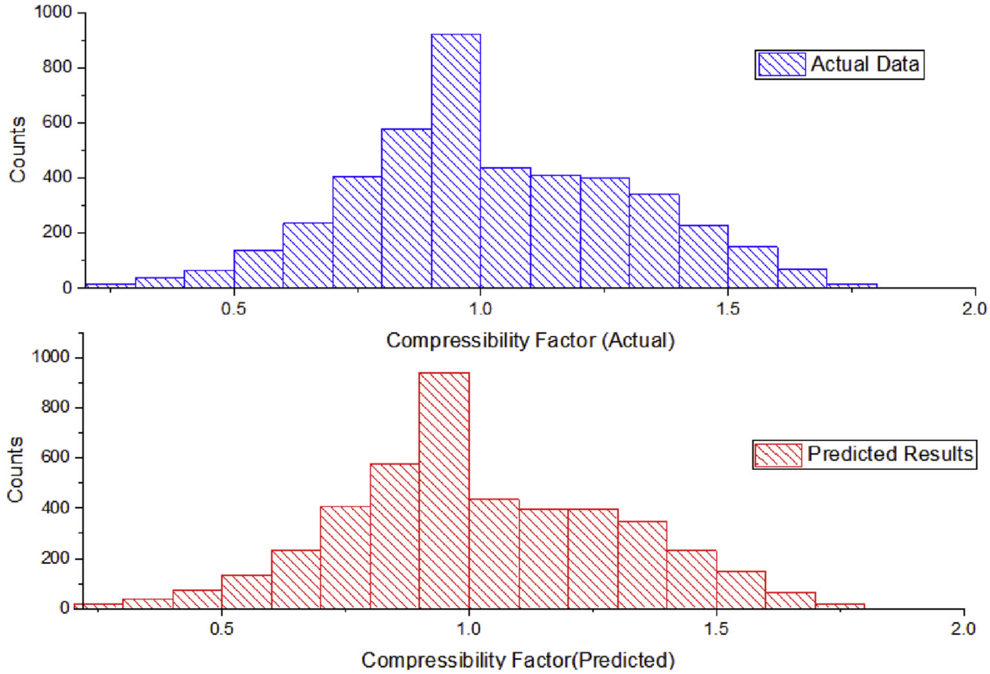

Fig. 2. Histogram of experimental and predicted z-factors.

4. Results and discussion

Table 3 gives the statistical parameters common to both the experimental and predicted data. The arithmetic means, geometric mean, median, the coefficient of variation, mean absolute deviation of both the predicted and actual data set are very similar. A closer look at the distribution (Fig. 2) of both the actual and predicted compressibility factor values shows that the prediction results mimics quite well the experimental data.

Table 4 shows the summary of the statistical performance metrics of the most accurate of all the explicit correlations that are devoid of any discontinuity along the isothermal lines. The table shows that the proposed correlation gives the highest and best correlation coefficient when compared to others.

Fig. 3a shows that the proposed correlation gives the smallest average absolute relative error values. While Azizi et al. [3] correlation gave the worst result using this metric. Fig. 3b shows the root mean square error values obtained by the six predictor models. The new correlation again shows its superiority by having an RMSE value of less than 1%.

Fig. 4a shows the maximum absolute percentage error. The new correlation is the best performer based on this indicator of performance as it has a maximum relative error below 30% while the other correlations have relatively higher error metrics. As shown in Fig. 4b, the proposed model has very low SSE values and hence performed better than the other correlations.

Figs. 5–8 shows the plots of predicted and experimental compressibility factor values at pseudo-reduced temperatures of 1.05, 1.2, 1.5, and 2.0. Closer to the unity pseudo-critical temperature (Tpr = 1.05), the proposed model shows that it can predict better than the other correlations. Away from the unity pseudo-critical temperature, the new equation still maintained its position as the best performer consistently.

Table 4
Statistical performance metrics of the explicit correlations.

	AAPE, (%)	MAPE, (%)	R2	RMSE	SSE
Shell Oil Co. (2004)	0.8126	38.4857	0.9987	0.0155	1.0698
Kareem (2016)	0.7869	67.1433	0.9993	0.0107	0.5109
Kamari et al (2016)	4.3991	105.2300	0.9893	0.0491	10.7600
Beggs & Brill (1973)	1.9869	70.5789	0.9964	0.0248	2.7409
Azizi (2017)	8.4368	284.0660	0.9581	0.1017	46.1231
This study	0.6794	27.7484	0.9997	0.0077	0.2659

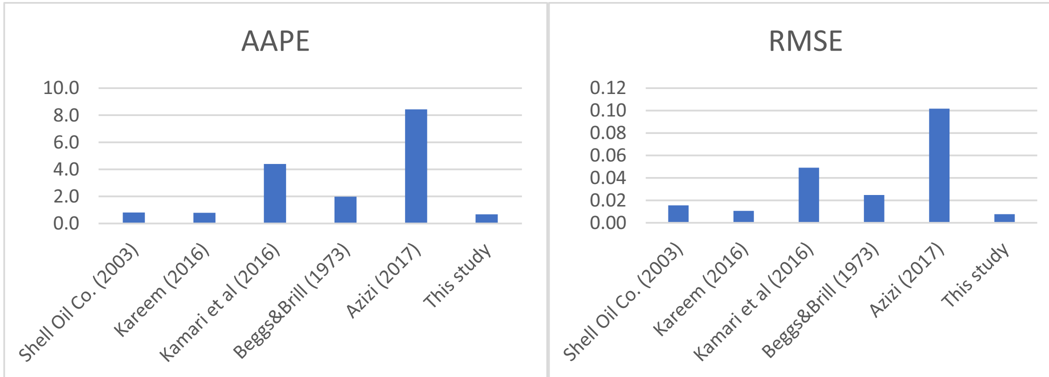

Fig. 3. (a) AAPE and (b) RMSE of six explicit correlation using 4455 S–K data points.

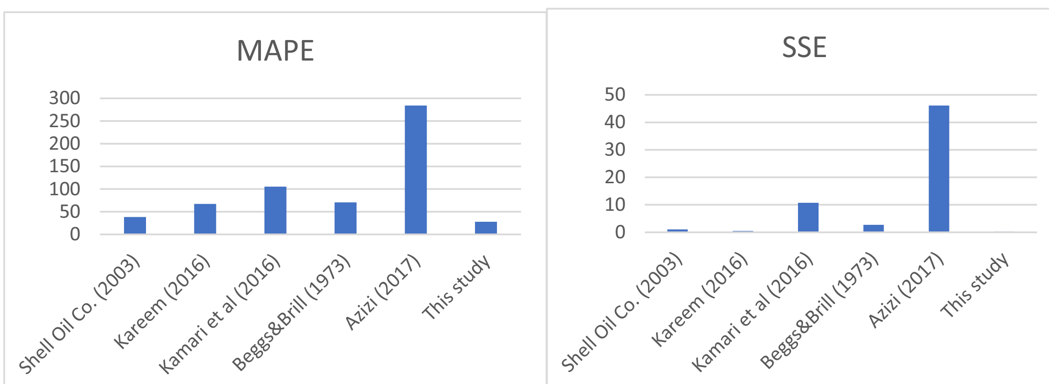

Fig. 4. (a) MAPE and (b) SSE of six explicit correlation using 4455 S–K data points.

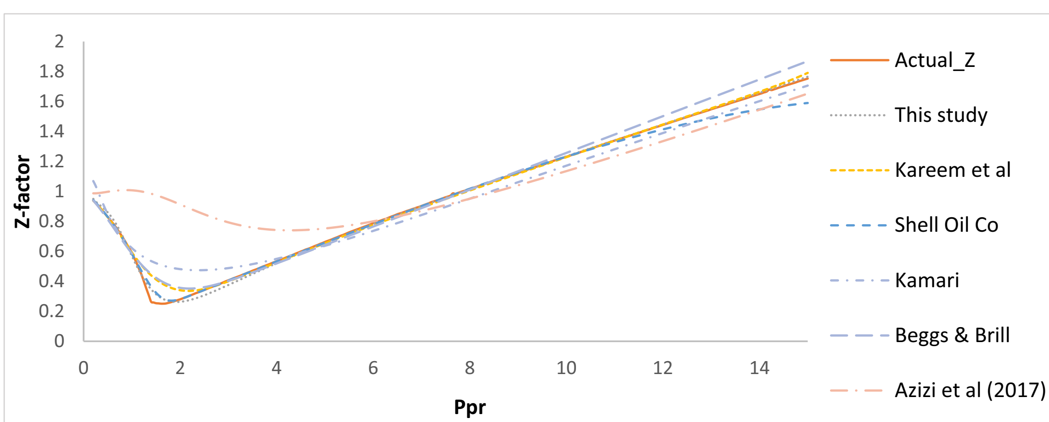

Fig. 5. Plot of z-factor for different correlations and experimental values at Tpr = 1.05.

4.1. Testing/validation

In order to test the robustness of the proposed correlation, more than ten percent of the original dataset that was excluded from the training dataset originally used for developing the algorithm was used for testing the proposed correlation. The testing dataset was also within the range of validity of the training dataset. Fig. 9 proves the robustness of the developed correlation. The proposed correlation not only gave a perfect match with the 45-degree line but also gave the highest correlation coefficient and the lowest root mean square errors.

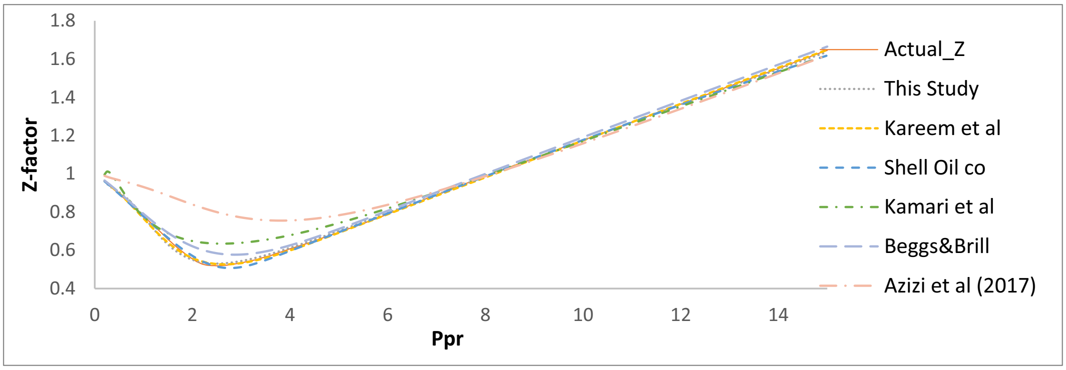

Fig. 6. Plot of z-factor for different correlations and experimental values at Tpr = 1.2.

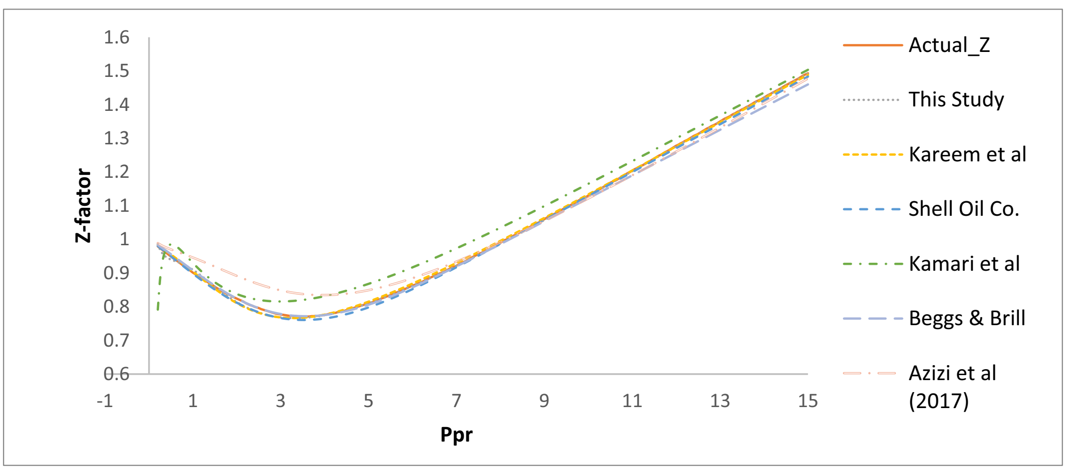

Fig. 7. Plot of z-factor for different correlations and experimental values at Tpr = 1.5.

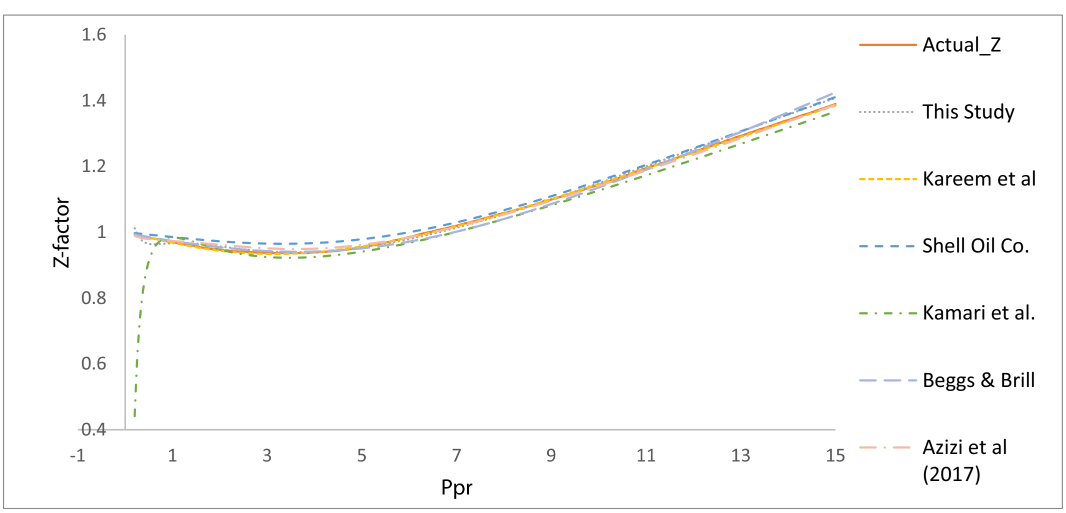

Fig. 8. Plot of z-factor for different correlations and experimental values at Tpr = 2.0.

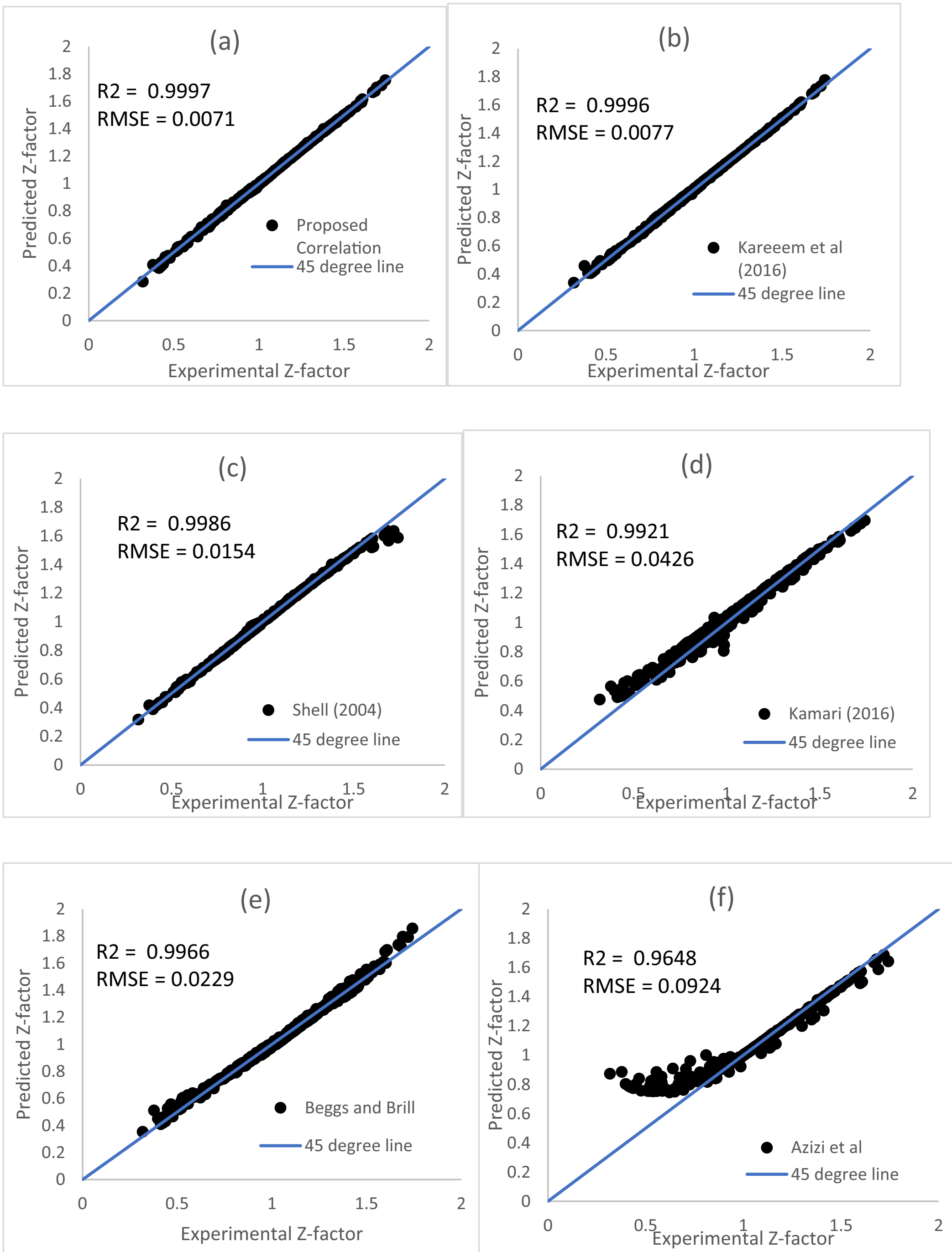

Fig. 9. Comparison of experimental and different correlation predictions using the test dataset.

5. Conclusion

The following deductions can be made from this study.

- A novel, simple yet robust and accurate explicit correlation has been developed.
- This model was developed based on a hybrid optimization technique using LMA-ODR model approach from a huge data set.
- Rigorous statistical analysis and comparison with other explicit models have been conducted.
- This new model has proven to be quite accurate and outperformed the other correlations considered within this wide range of pressure and temperature applications.

Conflicts of interest

The authors declare that there is no conflicts of interest.

Nomenclature

Ppr	pseudo-reduced pressure, and
Tpr	pseudo-reduced temperature
z	deviation factor
RMSE	root mean squared error
SSE	sum of squared errors of prediction
R2	Correlation Coefficient
MAPE	Maximum absolute percentage relative error
P	Pressure in (psi)
T	Temperature (R)
S−K	Standing and Katz
LMA	Levenberg-Marquart Algorithm
P_c	Critical pressure
T_c	Critical temperature

References

[1] Ahmed T. Reservoir engineering HandBook. 3rd ed. Elsevier Inc; 2006.
[2] Azizi N, Behbahani R & Isazadeh MA. An efficient correlation for calculating compressibility factor of natural gases. J Nat Gas Chem 2010;19:642−5. https://doi.org/10.1016/S1003-9953(09)60081-5.
[3] Azizi N & Behbahani RM. Predicting the compressibility factor of natural gas. Pet Sci Technol 2017;35:696−702. https://doi.org/10.1080/10916466.2016.1270305.
[4] Kareem LA, Iwalewa TM & Al-Marhoun M. New explicit correlation for the compressibility factor of natural gas: linearized z-factor isotherms. J Pet Explor Prod 2016;6:481−92. https://doi.org/10.1007/s13202-015-0209-3.
[5] Brill J & Beggs H. A study of two-phase flow in inclined pipes. Tulsa, Okla.: The University of Tulsa; 1973.
[6] Dranchuk PM, Purvis RA & Purvis RA. Computer calculations of natural gas compressibility factors using the standing and Katz correction. No. IP 74-008. 1974.
[7] Dranchuk PM & Abou-Kassem J. Calculation of Z-factors for natural gases using equation-of-state. J Can Pet Technol 1975;34−6.
[8] Kay WB. Density of hydrocarbon gases and vapors at high temperature and pressure. Ind Eng Chem 1936;1014−9.
[9] Stewart W, Burkhardt S & Voo D. Prediction of pseudocritical parameters for mixtures. In: AIChE Meet., Kansas City; 1956.
[10] Sutton R. Compressibility factors for high-molecular-weight reservoir gases. In: Annual technical conference exhibition SPE; 1985. https://doi.org/10.2118/14265-MS.
[11] Corredor J, Piper L & McCain WD. Compressibility factors for naturally occurring petroleum gases. In: 67th Annual technical conference exhibition SPE, Washington, DC; 1992.
[12] Carr NL, Kobayashi R & Burrows DB. Viscosity of hydrocarbon gases under pressure. J Pet Technol 1954;6:47−55. https://doi.org/10.2118/297-G.
[13] Wichert E & Aziz K. Calculate Z's for sour gases. Hydrocarb Process 1972:119−22.
[14] Poettmann FH & Carpenter P. The multiphase flow of gas, oil, and water through vertical flow strings with application to the design of gas-lift installations. Drill Prod Pract 1952;257. American Petroleum Institute.
[15] Kanzow C, Yamashita N & Fukushima M. Levenberg-Marquardt methods with strong local convergence properties for solving nonlinear equations with convex constraints. J Comput Appl Math 2005;173:321−43. https://doi.org/10.1016/j.cam.2004.03.015.
[16] Kenneth B & Frankford L. A method for the solution of certain. Non-Linear 1943;1:536−8.
[17] Zhou W. On the convergence of the modified Levenberg−Marquardt method with a nonmonotone second order Armijo type line search. J Comput Appl Math 2013;239:152−61. https://doi.org/10.1016/j.cam.2012.09.025.
[18] Ekechukwu G, Eliebid M & Falode O. Prediction of natural gas compressibility factor using artificial intelligence techniques. Pet Sci Technol 2019. https://doi.org/10.1080/10916466.2019.1599928. In Press.
[19] Boggs PT & Rogers JE. Orthogonal distance regression (NISTIR 89-4197). 1989. Nistir 89-4197.
[20] Poch J & Villaescusa I. Orthogonal distance regression: a good alternative to least squares for modeling sorption data. J Chem Eng Data 2012;57:490−9. https://doi.org/10.1021/je201070u.
[21] Kumar N. Compressibility Factors for Natural and Sour Reservoir Gases by Correlations and Cubic Equations of State. MS Thesis. Lubbock, Tex, USA: Texas Tech University; 2004.
[22] Standing MB & Katz DL. Density of natural gases. Trans. AIME 1942;146(01):140−9.
[23] Kamari A, Gharagheizi F, Mohammadi AH & Ramjugernath D. A corresponding states-based method for the estimation of natural gas compressibility factors. J. Mol. Liq. 2016;216:25−34. https://doi.org/10.1016/j.molliq.2015.12.103.